communications biology

A Nature Portfolio journal

Article

https://doi.org/10.1038/s42003-025-07874-7

A glutamatergic innervation from medial area of secondary visual cortex to lateral posterior thalamic nucleus facilitates nociceptive and neuropathic pain

Bei Tan[1,3], Xueqing Wu[1,3], Yila Ding[1,3], Cunrui Yuan[1,3], Yan Jin[2], Cenglin Xu[1], Tingting Hu[1], Jie Yu[1,2,4], Yu Du[1,4] & Zhong Chen[1,4]

Neuropathic pain involves complex cortical mechanisms, yet the role of the medial secondary visual cortex (V2M) remains poorly understood. We hypothesized that glutamatergic neurons in V2M ($V2M^{Glu}$) contribute to pain modulation and explored their functional involvement in both normal and neuropathic pain states. Here, we found that $V2M^{Glu}$ could be activated by peripheral stimulation under normal conditions. Optical inhibition or activation of unilateral $V2M^{Glu}$ respectively decreased or increased bilateral nociceptive sensitivity, with activation also inducing aversive emotions. Tracing experiments revealed that $V2M^{Glu}$ sends dense synaptic projections to the lateral posterior thalamic nucleus (LP) and lateral dorsal thalamic nucleus (LD). Notably, only optical manipulation of $V2M^{Glu}$ terminals in LP, rather than LD, affected bilateral pain perception. Following partial sciatic nerve ligation (PSL), $V2M^{Glu}$ exhibited hyperactivity, including increased spontaneous spike frequency and heightened responses to stimulation. Inhibiting $V2M^{Glu}$ alleviated PSL-induced mechanical allodynia, thermal hyperalgesia, and negative affective states related to pain. Inhibition of $V2M^{Glu}$ terminals in LP mitigated neuropathic pain. Here, we identified $V2M^{Glu}$ and its circuits to LP as part of the endogenous pain modulatory network, hyperactive after peripheral nerve injury and contributing to neuropathic pain. Our findings support targeting $V2M^{Glu}$ and related circuits as potential therapeutic strategies for neuropathic pain.

Neuropathic pain, a chronic condition stemming from damage to the somatosensory nervous system, affects a substantial segment of the population[1,2]. Characterized by spontaneous pain, dysesthesia, hyperalgesia, and allodynia, it often coexists with anxiety and depression, severely compromising patients' quality of life[3,4]. Conventional analgesics frequently provide limited relief and can produce intolerable side effects[5]. Consequently, deeper insights into the pathogenic mechanisms of neuropathic pain to identify new strategies and therapeutic targets are ungently demanded.

Extensive research has revealed that neuronal sensitization in the peripheral and central nervous system (CNS) contributes to the development of neuropathic pain. Within the CNS, nerve injury-induced plasticity changes always occur in cortical and subcortical regions, affecting diverse neural circuits that are involved in the initiation, maintenance and modulation of pain. For instance, studies have identified that specific modulation of different subregions within the midcingulate cortex (MCC) can bidirectionally regulate pain sensitivity[6]. Nuclei, located in the prefrontal cortex and posterior insular cortex, are believed to participate in the spatial discrimination and intensity encoding of pain perception[7,8]. Moreover, magnetic resonance imaging has shown significantly enhanced activity in the somatosensory cortex and cingulate cortex in patients with neuropathic pain[9]. Beyond the nociceptive aspect, persistent pain also induces negative emotions and comorbid affective disorders, such as anxiety and depression, which are also connected to the function of anterior cingulate cortex and anterior insular cortex[10,11].

[1]Key Laboratory of Neuropharmacology and Translational Medicine of Zhejiang Province, College of Pharmaceutical Sciences, Zhejiang Chinese Medical University, Hangzhou, China. [2]The Second Affiliated Hospital of Zhejiang Chinese Medical University, Xinhua Hospital of Zhejiang Province, Hangzhou, China. [3]These authors contributed equally: Bei Tan, Xueqing Wu, Yila Ding, Cunrui Yuan.[4]These authors jointly supervised this work: Jie Yu, Yu Du, Zhong Chen. e-mail: chenzhong@zju.edu.cn

Recent research has broadened to sensory-processing regions like the visual cortex as potential targets for non-invasive pain therapies. Phototherapy, particularly green light exposure, has relieved pain in fibromyalgia and migraine patients[12,13]. Bright light treatment exhibits antinociceptive effects in mice by activating the retina-vLGN/IGL-l/vlPAG pathway[14]. Our previous work established that the ventral lateral geniculate nucleus (vLGN) differentially modulates neuropathic pain: green light-activated vLGN glutamatergic neurons produce analgesia, while red light-activated GABAergic neurons induce hyperalgesia[15]. Based on these findings, we hypothesize that the visual cortex and its associated neural circuits play a significant role in pain modulation. In addition, studies report enlarged V2 volumes and enhanced nociceptive-driven blood flow in neuropathic models, as well as stronger connectivity between V2 and somatosensory areas. In non-human primates with trichromatic vision, neuron clustering is more pronounced in V2 than the primary visual cortex (V1), suggesting a peak density of cells responsive to green hues[16]. In migraine patients, V2 shows significantly stronger connectivity with the primary (S1) and secondary (S2) somatosensory cortices[17]. Additionally, the medial area of V2 (V2M) is involved in translating visual input into motor actions, and its functional connectivity with the periaqueductal gray (PAG) increases during visual-induced analgesia, hinting at its modulatory role in pain[18,19]. Despite these observations, the precise role of V2M and its circuits in the modulation of neuropathic pain remains largely unexplored. This study aims to investigate the functional involvement of glutamatergic neurons in V2M, focusing on their contribution to pain perception and emotional responses to pain, and to elucidate the underlying neural mechanisms that may offer new therapeutic targets for neuropathic pain.

In this article, we report that $V2M^{Glu}$ becomes hyperactive following peripheral nerve injury, contributing to neuropathic pain. These neurons facilitate pain perception through corticothalamic projections to the LP, but not the LD. This finding clarifies the role of V2M ($V2M^{Glu}$) in neuropathic pain and provides new potential targets for precise clinical interventions.

Results

Nerve injury activates glutamatergic neurons in the V2M

To investigate whether V2M are involved in pain processing, we examined the c-Fos expression, a well-validated marker of neuronal activation[20], in the visual cortical regions, including the V1, the lateral and medial of V2 (V2L and V2M), and the retrosplenial agranular cortex (RSA) on day 14 after sham or PSL surgery. The results showed a pronounced upsurge of c-Fos expression within the V2M, compared to the sham group, but no significant change in the V1, V2L, or RSA in the PSL group (Fig. 1A–C). Intense c-Fos^{+} neurons identified in the V2M were highly overlapped with CaMKIIα (Fig. 1D, E), indicating that the majority of nerve injury-activated neurons in V2M are glutamatergic neurons ($V2M^{Glu}$). Then, we have conducted in vivo single unit recording of $V2M^{Glu}$ in anesthetized mice, with or without a pinch stimulus to the hind paw of mice. Characteristic neuronal discharge was used to distinguish glutamatergic neurons (Fig. 1F). The recording results showed that the spontaneous spikes firing rates of $V2M^{Glu}$ were increased following PSL surgery (Fig. 1G). Three distinct response patterns-activating, inhibiting, and no response of $V2M^{Glu}$ to noxious pinch stimulation were observed. As for the sham group, around half of the $V2M^{Glu}$ were activated by pinch stimuli, resulting in a heightened average firing rate of all recorded $V2M^{Glu}$ during noxious stimulation (Fig. 1H–J). Notably, a greater proportion (~ 67%) of recorded $V2M^{Glu}$ neurons were activated by pinch stimuli in PSL mice, leading to a significant elevation of the average spike-firing frequency during noxious stimulation (Fig. 1H–J). These findings suggest that $V2M^{Glu}$ is responsible and sensitive to peripheral noxious stimuli under both physiological conditions and chronic pain. Following sciatic nerve injury, $V2M^{Glu}$ behave hyperactivated and exhibit an enhanced responsiveness to noxious stimuli.

To further determine whether $V2M^{Glu}$ is involved in pain processing, we examined the activity of $V2M^{Glu}$ by fiber photometry, between control and PSL animals. We microinjected AAV-CaMKIIα-GCAMP6s-eYFP into the V2M and used a calcium imaging fiber recording system to monitor the real-time neuronal activity of $V2M^{Glu}$ in the awake C57BL/6 mice (Fig. 2A, B). In the PSL group, the calcium signal of $V2M^{Glu}$ showed a pronounced elevation in response to hind paw pinch, von Frey hairs and hargreaves stimulations (Fig. 2C–H). In contrast, unlike the results from single-cell recordings, the $V2M^{Glu}$ from sham group did not exhibit any evident changes in calcium signaling with peripheral noxcious stimuli. These results indicate that after nerve injury induced by PSL surgery, $V2M^{Glu}$ becomes hyperactivated, with responding to noxious stimuli, including mechanical and thermal stimuli, and may play a vital role in neuropathic pain.

Selective activation of $V2M^{Glu}$ promotes pain under physiological conditions

Next, optogenetic modulation was used to investigate the regulation of $V2M^{Glu}$ activity on abnormal nociception. AAV-CaMKIIα-eArch3.0-eYFP virus selectively targeting glutamatergic neurons was infused into the V2M (Fig. 3A). The functional transduction of virus in these neurons was verified by the co-localization of eYFP with CaMKIIα and the reduction of firing by yellow laser illumination (Fig. 3B, C). The results showed that selective inhibition of $V2M^{Glu}$ with yellow light significantly increased the mechanical withdrawal threshold and thermal withdrawal latency of the bilateral hind paw of intact naive mice (Fig. 3E, F). However, in the RTPP test, there was no different of the time that mice spent between the yellow light-paired and unpaired box (Fig. 3G, H). These results indicates that the inhibition of $V2M^{Glu}$ activity suppressed the nociceptive perception in naïve animals, but does not induce any place preference (rewarding) or avoidance (aversive) emotions.

Then, we examined the effect of $V2M^{Glu}$ activation on pain and mood status by using AAV-CaMKIIα-ChR2-eYFP virus, which was verified by the increase of neuronal firing on blue laser illumination (Fig. 3D). As expected, the results showed that optical activation of $V2M^{Glu}$ decreased the mechanical withdrawal threshold and thermal withdrawal latency of the bilateral hind paw (Fig. 3I, J), indicating a pain facilitation in naive mice. Moreover, different from the effect of inhibition by yellow light, activation of these neurons by blue light induced place avoidance to the light-paired chamber (Fig. 3K, L), supporting that $V2M^{Glu}$ activation induced pain-associated negative mood under physiological conditions.

Selective inhibition of $V2M^{Glu}$ relieves neuropathic pain

As mentioned above, the firing rate of $V2M^{Glu}$ significantly, as well as calcium signaling, responsively increased, and more $V2M^{Glu}$ was activated by noxious stimuli in the PSL mice, indicating a hyperactivity of $V2M^{Glu}$ after nerve injury (Fig. 1). To determine the role of hyperactive $V2M^{Glu}$ in neuropathic pain, we further investigated the effect of specific manipulation of $V2M^{Glu}$ on neuropathic pain. First, AAV-CaMKIIα-eArch3.0-eYFP virus was injected into the V2M where the soma of $V2M^{Glu}$ located, and PSL surgery was performed three weeks later (Fig. 4A, B). Yellow light was appliecated into the V2M and the behavioral results showed that, in comparison to the control group, light-induced inhibition of $V2M^{Glu}$ activity reduced mechanical allodynia and thermal hyperalgesia, evidenced by a notable rise in mechanical withdrawal threshold and thermal withdrawal latency in both hind paws on D7 and D14 (Fig. 4C, D), which indicates that hyperactive $V2M^{Glu}$ following nerve injury contribute to neuropathic pain, and thus their inhibition has a therapeutic effect. Notably, in the CPP test, we observed that optical inhibition of $V2M^{Glu}$ induced place preference in neuropathic mice (Fig. 4G–I), suggesting hyperactive $V2M^{Glu}$ neurons may be involved in the negative emotions that are associated with continuous spontaneous pain after sciatic nerve injury.

Conversely, further experiments showed that activation of $V2M^{Glu}$ using blue laser light did not affect bilateral mechanical withdrawal threshold and thermal withdrawal latency in neuropathic mice treated with AAV-CaMKIIα-ChR2-eYFP virus that targeting glutamatergic neurons (Fig. 4E, F). Similarly, the CPP test revealed no changes either in the time spent in the chamber associated with blue light (Fig. 4G–I). These findings suggest that optical activation of hyperactive $V2M^{Glu}$ following nerve injury

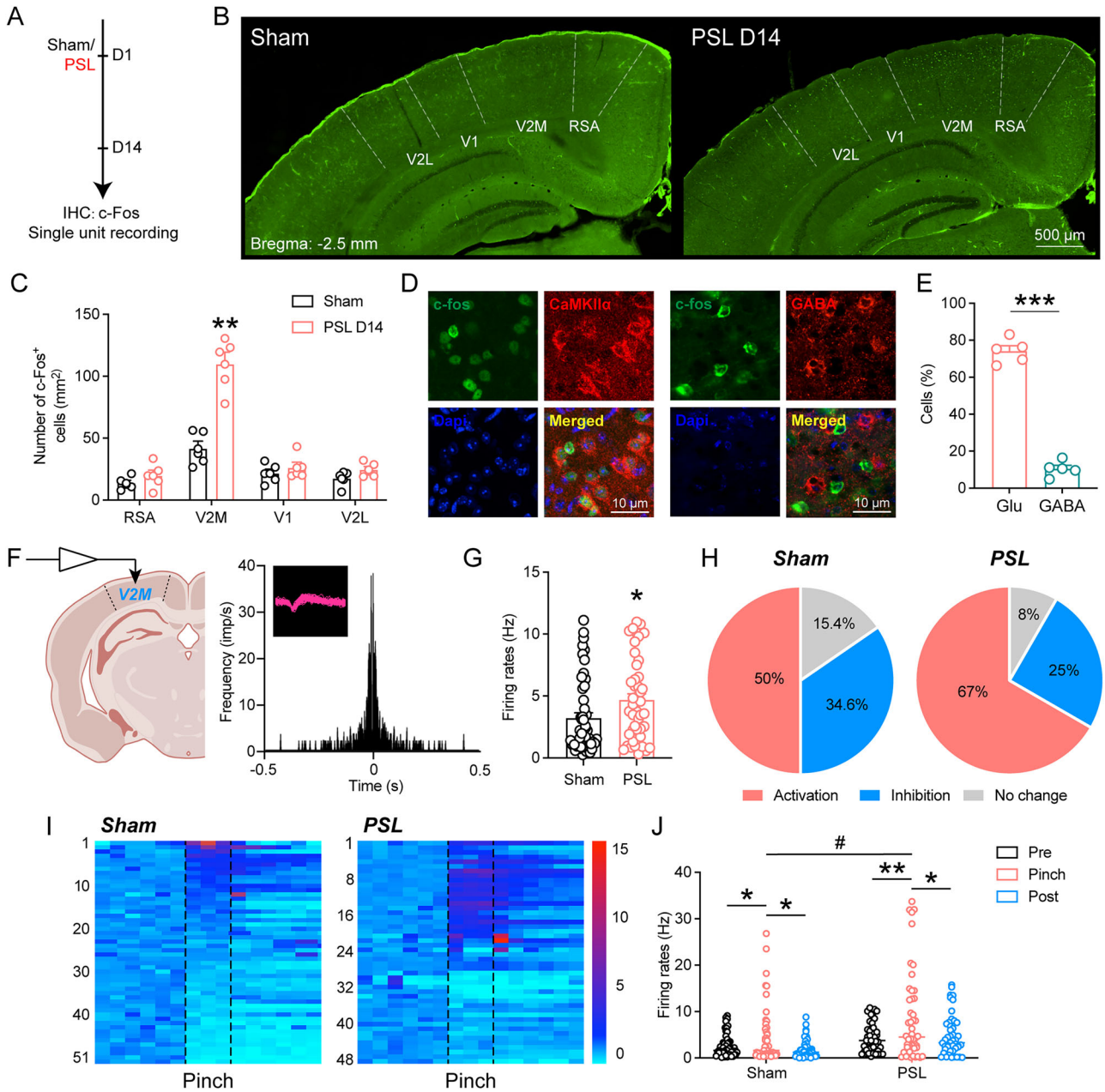

Fig. 1 | The V2M^{Glu} is hyperactive following PSL. A Timeline of experimental procedure. **B** Photomicrographs showing c-Fos$^+$ expression in the visual cortex. **C** The number of c-Fos$^+$ cells in RSA, V2M, V1 and V2L in sham and PSL mice. $n = 6$ mice. **D** Photomicrographs showing the co-localization of c-Fos$^+$ with CaMKIIα (left) and GABA (right) in the V2M. **E** Percentage of c-Fos$^+$ neurons co-labeled with CaMKIIa or GABA. $n = 5$ mice. **F** Schematic drawing of the electrode placement (left) in the left V2M and the waveform and autocorrelation of a representative glutamatergic neuron (right). **G** Firing rates of spontaneous firing in sham and PSL mice. $n = 40$ from 10 mice. **H** Proportion of V2M^{Glu} that showed increase, decrease and no change in firing frequency upon hind paw pinch stimulation in sham and PSL mice. **I** The heatmaps of firing frequency in sham or PSL mice pre, during and post pinch stimuli. **J** Firing frequency of V2M^{Glu} pre and during pinch stimulation in sham and PSL mice. $n = 48$-51 from 10 mice. Significance was calculated by means of t-test in **C**, **E**, **G**; one-way ANOVA with Tukey's post hoc test in J. $^*p < 0.05$, $^{**}p < 0.01$ and $^{***}p < 0.001$, respectively, sham versus PSL, pre or post versus pinch. $\#p < 0.05$, sham pinch versus PSL pinch. All data are presented as mean ± SEM.

with the current parameters neither exacerbate pain-like behiviours, nor the associated aversions.

Projection to the LP mediate the pain modulatory role of V2M^{Glu}

Numerous studies have reported that projections from the cortex to the thalamus are involved in the modulation of pain[21,22]. We then set out to determine whether the pain modulatory role of V2M^{Glu} is fulfilled by any of these corticothalamic projections. Anterograde virus AAV-CaMKIIα-Arch-EYFP was first injected into the V2M. Three weeks later, EYFP were observed in the thalamus, including LD and LP (Fig. 5), indicating a glutaminergic innavation from V2M to both LD and LP.

Considering the key position of LP and LD in pain signals transmission and modulation, we postulated that V2M^{Glu} might modulate pain by projecting to the LP and/or LD. Therefore, we selectively manipulated the glutamatergic circuits from the V2M to LP and LD, respectively, to dissect their roles in pain modulation. AAV-CaMKIIα-eArch3.0-eYFP or AAV-CaMKIIα-ChR2-eYFP virus that selectively targeting glutamatergic neurons was infused into the V2M and the optical fibers were implanted into LP and LD to selectively manipulate the V2M^{Glu}-LP (Fig. 6) and V2M^{Glu}-LD circuits in naïve animals (Fig. 7). As expected, the results showed that selective optical inhibition of glutamatergic axon terminals from V2M to LP significantly elevated the mechanical pain threshold and thermal

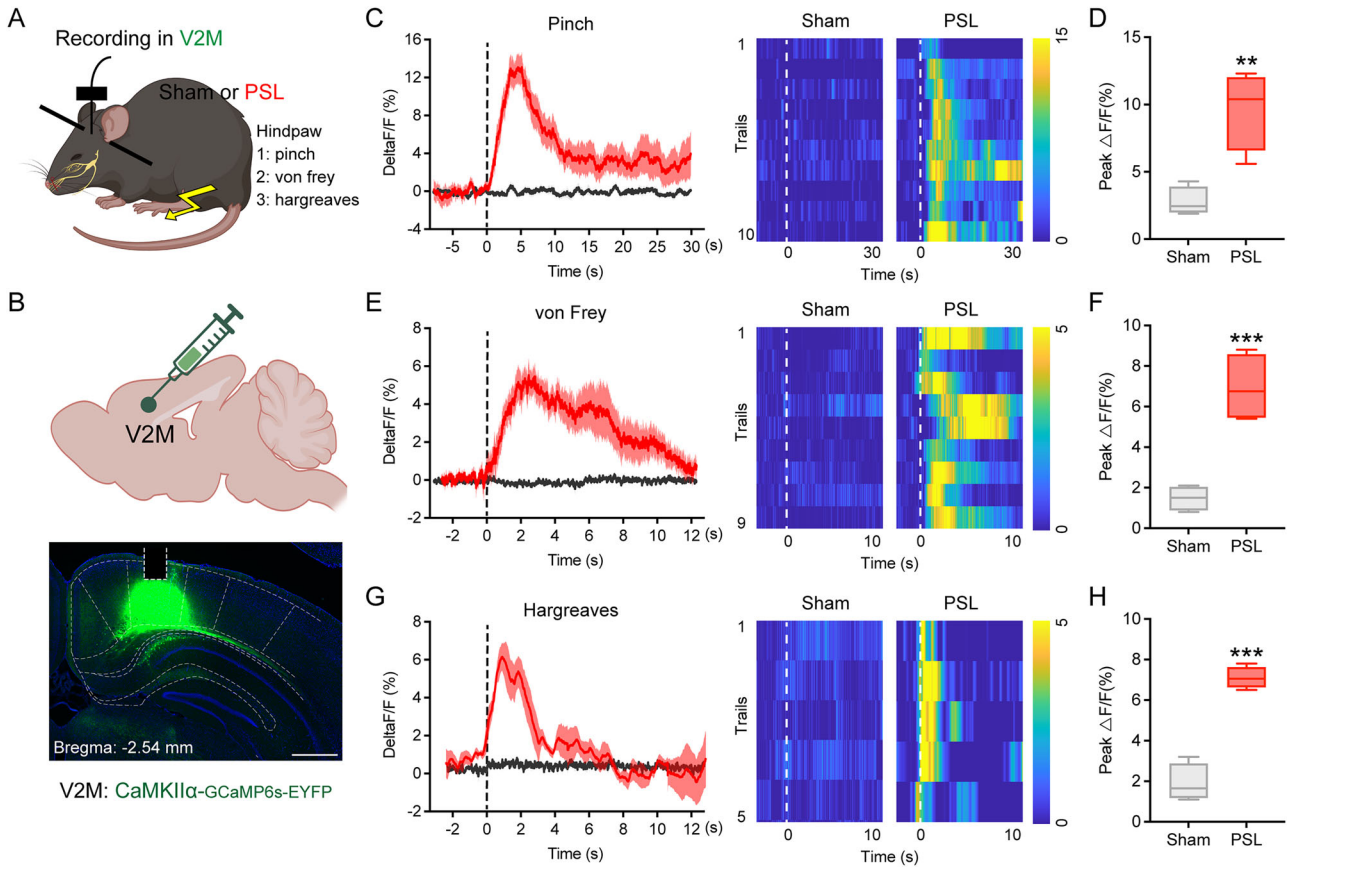

Fig. 2 | The V2M^{Glu} is excited by peripheral noxious stimulation. **A** Schematic drawing of the fiber photometry setup and different kinds of stimuli applied on the hind paw. **B** Schematic and photomicrograph showing of the AAV-CaMKIIα-GCaMP6s-EYFP injection in V2M. Bar = 500 μm. **C** Peri-event plot and heatmaps of GCaMP6s Δ*F*/*F* after hind paw pinch stimuli. **D** Peak Δ*F*/*F* while pinch stimulation delivered of sham and PSL mice. $n = 4$. **E** Peri-event plot and heatmaps of GCaMP6s Δ*F*/*F* after hind paw von Frey stimulation. **F** Peak Δ*F*/*F* while von Frey stimulation delivered of sham and PSL mice. $n = 4$. **G** Peri-event plot and heatmaps of GCaMP6s Δ*F*/*F* after hind paw hargreaves stimulation. **H** Peak Δ*F*/*F* while hargreaves stimulation delivered of sham and PSL mice. $n = 4$. Significance was calculated by means of t-test in **D**, **F**, **H**. $^{**}p < 0.01$ and $^{***}p < 0.001$, respectively, sham versus PSL. All data are presented as mean ± SEM.

withdrawal latency of the bilateral hind paws in naive mice (Fig. 6A–C). By contrast, selective optical activation of glutamatergic axon terminals from V2M to LP significantly reduced the mechanical pain threshold and thermal withdrawal latency, indicating that activation of the glutamatergic circuit from the V2M to LP facilitates nociception (Fig. 6D, E). As for RTPP tests, contrast ot the effect of inhibition by yellow light, activation of V2M^{Glu}-LP by blue light induced place avoidance to the light-paired chamber (Fig. 6F, G), supporting that V2M^{Glu} activation induced negative mood status under physiological conditions. These results demonstrate that the pain modulatory role of V2M^{Glu} is mediated by projections to the LP.

However, in another downstream regulatory loop of V2M involving LD, we discovered that neither yellow light nor blue light manipulation of V2M^{Glu} at LD that activated the V2M^{Glu} terminals affected any of the bilateral hind paw mechanical pain withdrawal threshold or thermal pain withdrawal latency in mice (Fig. 7). This finding suggests that the modulation of V2M nociceptive sensitivity under physiological conditions is not mediated through the LD downstream pathway.

Selective inhibition of the V2M^{Glu} to LP attenuates neuropathic pain

To further examine whether hyperactive V2M^{Glu} contributes to the neuropathic pain through the same corticothalamic circuits as that in physiological condition, we optically inhibited the terminals of V2M^{Glu} in the LP and LD in neuropathic mice, respectively (Fig. 8A, B). We found that photoinhibition of the terminals in the LP alleviated the mechanical and thermal pain, as well as associated aversive emotions (Fig. 8C–E). In the contrary, selective inhibition of glutamatergic nerve terminals from V2M to LD neither affected mechanical pain threshold, thermal withdrawal latency (Fig. 8F, G), nor induce preference in the CPP test (Fig. 8H) of PSL mice. These results demonstrate that the projections from V2M to the LP, but not to the LD, mediate the promotive role of hyperactive V2M^{Glu} in neuropathic pain. The above results suggest that V2M^{Glu} is involved in pain regulation under both physiological conditions and neuropathic pain, and this regulation is achieved through its neural circuitry connections to the LP.

Discussion

In this study, we demonstrated that peripheral noxious mechanical stimuli could activate approximately half of the glutamatergic neurons in the V2M area of the visual cortex under physiological conditions. Both of the excitability and responsive population of V2M^{Glu} significantly increased under neuropathic conditions. Using optogenetic techniques, we further demonstrated that inhibition of V2M^{Glu} raised, while activation lowered, the nociceptive and neuropathic pain threshold to mechanical and thermal stimuli. Additionally, activating V2M^{Glu} activity induced pain-associated aversive emotions in the RTPP test. These results collectively suggest that V2M^{Glu} actively participates in the modulation of pain perception and associated emotional states. To our knowledge, this is the first experimental evidence of V2M^{Glu}'s role in pain modulation.

Recently, the roles of auditory, olfactory, and visual stimuli in pain generation have become focal research topics. Studies have shown that specific sound frequencies, such as Mozart's symphonies, can modulate pain by altering excitability in the auditory cortex-to-thalamus pathway[23].

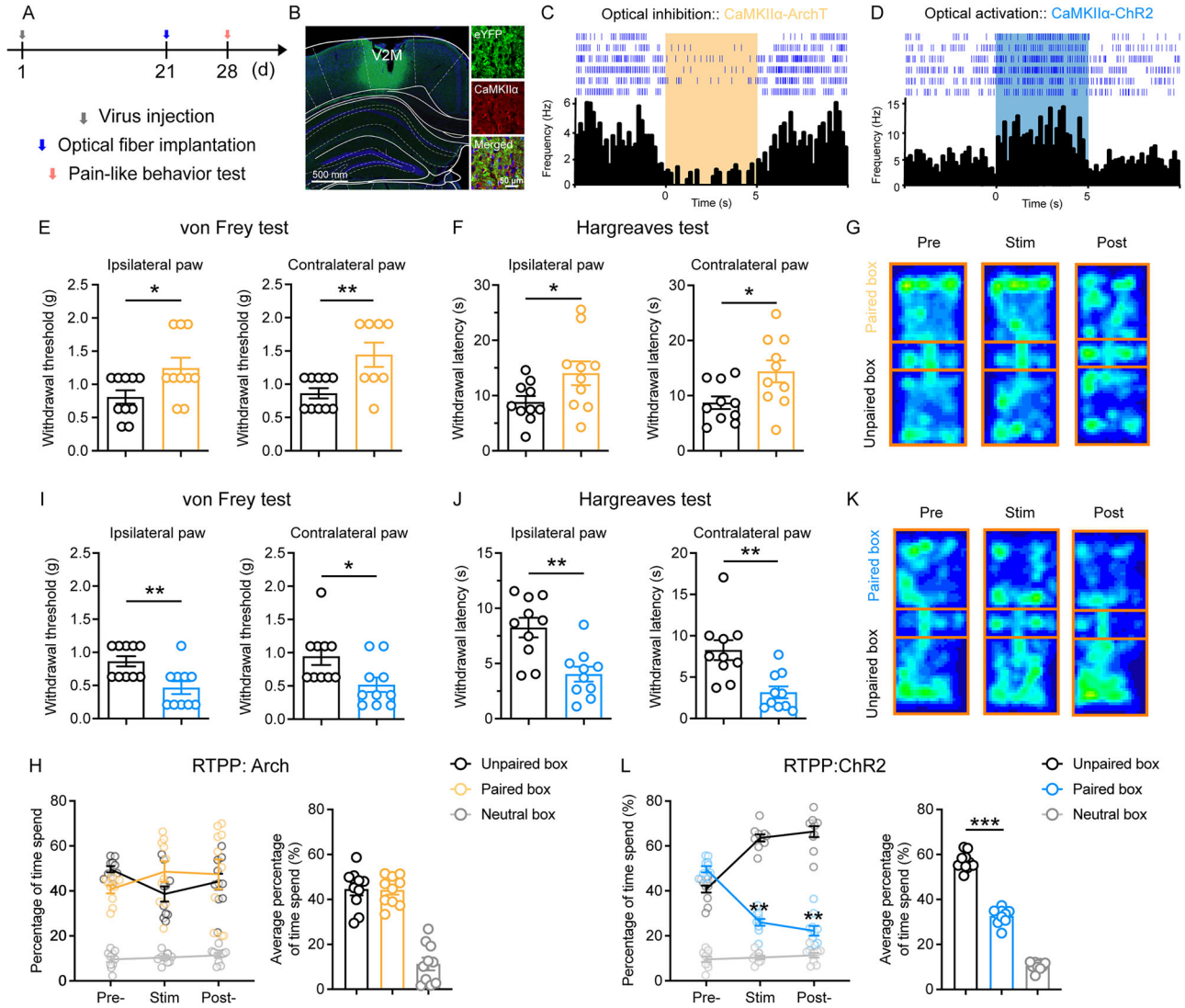

Fig. 3 | Selective manipulation of V2M^{Glu} modulates nociception. **A** Timeline of the experimental procedure. **B** Representative photomicrograph showing virus carrying eYFP and targeting glutamatergic neurons (CaMKIIα) were expressed and optical fiber was implanted in the V2M. (**C**) Example V2M^{Glu} with Arch virus that inhibited its firing frequency in response to yellow laser stimulation. **D** Example V2M^{Glu} with ChR2 virus that increased its firing frequency in response to blue laser stimulation. Optical inhibition of unilateral V2M^{Glu} inhibited bilateral mechanical (**E**) and thermal (**F**) nociception. $n = 10$. **G** Heatmaps of pre-, post- and during stimulation in RTPP. **H** The percentage of time spend (left), and average percentage of time spend (right) in yellow light paired, unpaired and neutral box. $n = 10$. Optical activation of unilateral V2M^{Glu} induced bilateral mechanical (**I**) and thermal (**J**) nociception. $n = 10$. **K** Heatmaps of pre-, post- and during stimulation in RTPP. **L** The percentage of time spend (left), and average percentage of time spend (right) in blue light paired, unpaired, and neutral box. $n = 10$. Significance was calculated by means of t-test in E, F, I, J, L and two-way ANOVA with Bonferroni's post hoc test in L. $^{*}p < 0.05$, $^{**}p < 0.01$ and $^{***}p < 0.001$, respectively, laser on versus laser off or unpaired box versus paired box. All data are presented as mean ± SEM.

Pleasant scents can alleviate negative emotions caused by pain, and migraine sufferers display enhanced sensitivity to olfactory stimuli mediated through the piriform cortex[24,25]. As for visual stimuli, as early as in 1992, scientists noted that observing the healthy arm through a mirror could relieve phantom limb pain[26]. Virtual reality, derived from visual stimuli, has been explored for treating conditions such as phantom limb pain and complex regional pain syndrome, suggesting that visual stimulation may have a pain modulatory effect and serve as an effective method for treating neuropathic pain[27]. In particular, the V2M, a crucial subregion within the visual cortex, has been implicated in analgesic treatments through enhanced effective connectivity between the V2 area and the PAG, a classical pain-related nucleus[28]. Although clinical imaging studies have reported activity changes across multiple cortical nuclei in neuropathic pain states[4], the involvement and disease relevance of V2M^{Glu} and their downstream circuits remain unclear. Our in vivo electrophysiological experiments revealed that, compared to physiological conditions, V2M^{Glu} in anesthetized mice post-PSL surgery exhibited hyperactivity and an increased activated response proportion to peripheral mechanical stimulation. Given that optical activation or inhibition of V2M^{Glu} respectively facilitated nociception or produced analgesic effects, it is reasonable to speculate that increased activity of V2M^{Glu} following nerve injury contributes to the abnormal pain sensitivity in PSL. This is supported by findings that optical inhibition of V2M^{Glu} alleviated bilateral mechanical allodynia and thermal hyperalgesia in PSL mice. Moreover, unlike what underphysiological conditions, the inhibition of V2M^{Glu} in the CPP test induced place preference, indicating that hyperactivity of V2M^{Glu} under neuropathic conditions might lead to spontaneous pain and/or pain-associated aversion. Although less prominent than in neuropathic conditions, approximately half of the V2M^{Glu} neurons can still be activated by peripheral noxious mechanical stimuli under physiological conditions. This finding suggests that V2M^{Glu} may enhance pain perception by increasing neuronal excitability. Under physiological conditions, the activity of these neurons helps maintain a normal

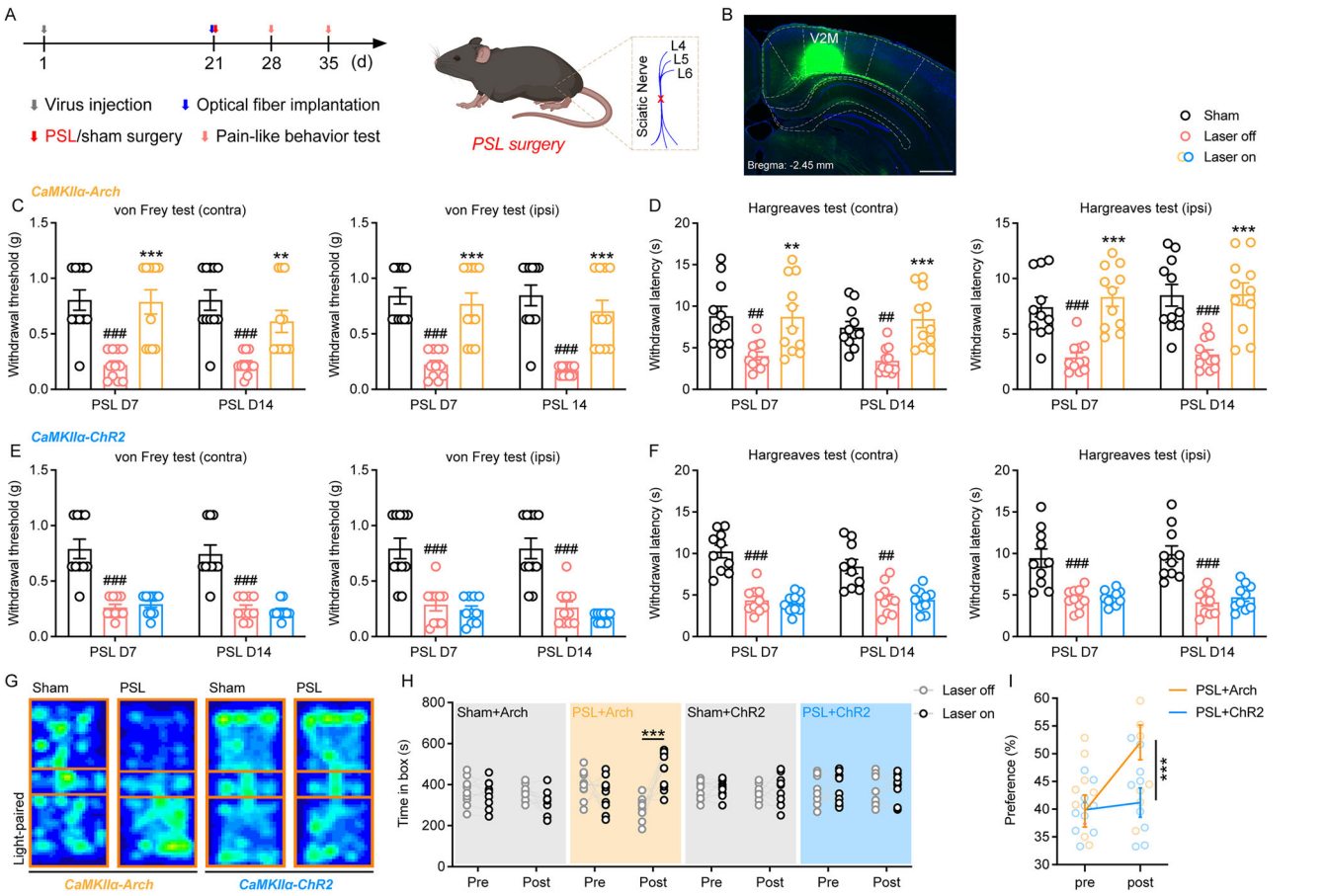

Fig. 4 | Selective inhibition of V2M^{Glu} alleviates neuropathic pain. A Timeline of experimental procedure. **B** Representative photomicrograph showing virus carrying eYFP and optical fiber was implanted in the V2M. **C**, **D** Withdrawal thresholds and withdrawal latency to mechanical and thermal stimulation of bilateral hind paw during optical inhibition of unilateral V2M^{Glu}. $n = 11$. **E**, **F** Withdrawal thresholds and withdrawal latency to mechanical or thermal stimulation of bilateral hind paw during optical activation of unilateral V2M^{Glu}. $n = 10$. **G** Representative heat maps in the CPP test. Time spends (**H**) and preference (**I**) by the mice in the laser off and laser on paired boxes in pre- and post-conditioning phases of Sham/PSL+ Arch/ChR2. $n = 10$. Significance was calculated by means of t-test in H and two-way ANOVA with Bonferroni's post hoc test in **C**–**F** and **I**. $^{**}p < 0.01$ and $^{***}p < 0.001$, respectively, laser on versus laser off in C-F and H, PSL+ Arch versus PSL+ ChR2 in I. $^{\#\#}p < 0.01$ and $^{\#\#\#}p < 0.001$, respectively, sham versus laser off in (**C**–**F**). All data are presented as mean ± SEM.

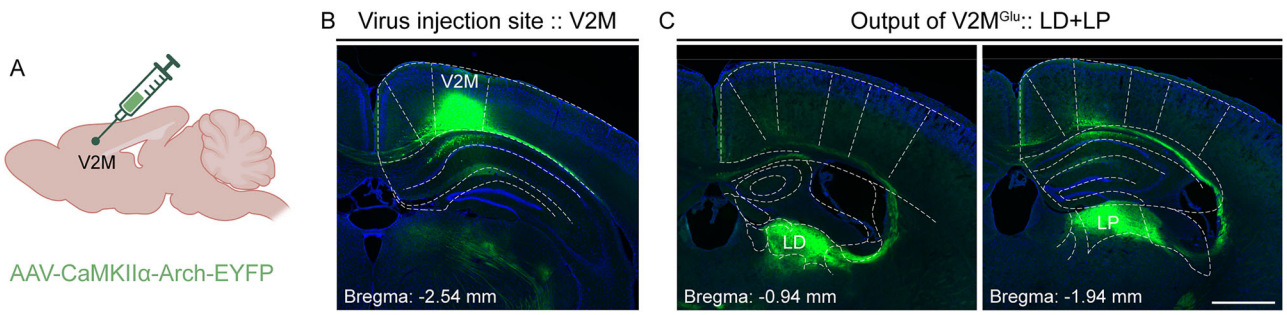

Fig. 5 | V2M^{Glu} projects to the thalamus. A Schematic of sites for anterograde trace virus injection in V2M. **B** Photomicrograph showing virus carrying eYFP and targeting glutamatergic neurons were infused in the V2M. **C** Photomicrographs showing axon terminals labeled with eYFP in the thalamus. LD laterodorsal thalamic nucleus, LP lateral posterior thalamic nucleus.

pain threshold. Moreover, our results also indicate that inhibition of these neurons under physiological conditions can upregulate pain thresholds and alleviate pain perception. Therefore, these findings highlight the important role of V2M^{Glu} in the endogenous pain modulatory network, where it exhibits bidirectional modulation properties, capable of both enhancing pain signals and alleviating pain through inhibition of its activity.

It is well established that projections from the cortex to the thalamus are extensive, even surpassing those from the thalamus to the cortex[29,30]. Research also indicates that these cortico-thalamic projections can significantly modulate the thalamic neurons' responses to peripheral stimulation[31,32]. Our anterograde tracing experiments confirmed that V2M^{Glu} sends dense monosynaptic projections to the ipsilateral thalamus, specifically to the LP and the LD, which are pivotal in pain processing. Further behavioral tests revealed that optogenetic inhibition of V2M^{Glu} terminals in LP suppressed, activation-facilitated, neuropathic pain. In contrast, manipulation of V2M^{Glu} in LD did not affect the pain

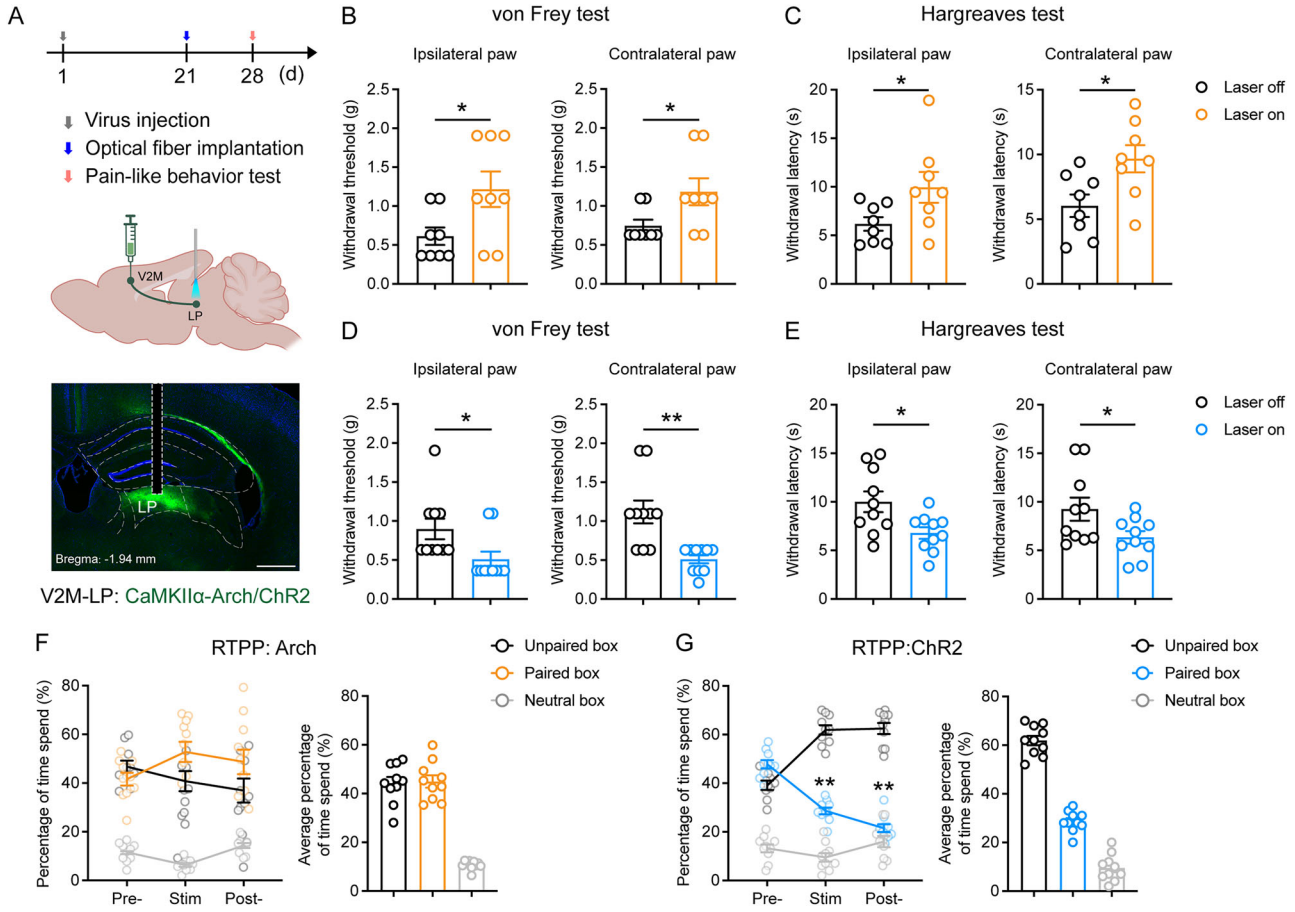

Fig. 6 | Selective inhibition of V2M^{Glu}-LP inhibited nociception. A Timeline of experimental procedure (upper), schematic of sites for virus injection and optical fiber implantation (middle) and photomicrograph showing the expression of eYFP and optical fiber implantation in the LP (lower). **B**, **C** Withdrawal thresholds and withdrawal latency to mechanical and thermal stimulation of bilateral hind paw during optical inhibition of terminals from V2M^{Glu} in LP. $n = 8$. **D**, **E** Withdrawal thresholds and withdrawal latency to mechanical and thermal stimulation of bilateral hind paw during optical activation of terminals from V2M^{Glu} in LP. $n = 10$. **F** The percentage of time spend (left), and average percentage of time spend (right) in yellow light paired, unpaired, and neutral box. **G** The percentage of time spend (left), and average percentage of time spend (right) in blue light paired, unpaired and neutral box. $n = 10$. Significance was calculated by means of t-test in **B**–**E** and two-way ANOVA with Bonferroni's post hoc test in G. $^{*}p < 0.05$, $^{**}p < 0.01$ and $^{***}p < 0.001$, respectively, laser on versus laser off in **B**-**E**, unpaired box versus paired box in G. All data are presented as mean ± SEM.

threshold. Although LP and LD are subregions of the thalamic nuclei, their location, upstream and downstream circuit connections, and their roles in physiological and pathological conditions differ[33,34]. LD were found to be important in learning and memory functions. For example, it has been noted that damage to LD affects pattern learning, leading to amnesia. LD neurons depend on visual cues to provide spatial positioning information to the hippocampus, playing a crucial role in spatial learning and memory[35]. Conversely, LP is closely associated with non-visual processing functions, including handling visual stimuli, executing visually guided behaviors, and eliciting reflex responses to threat/fear-related stimuli[36,37]. Functional abnormalities in LP can cause brain overexcitation, impacting parasympathetic and sympathetic nerve output, thereby contributing to systemic abnormal pain and photophobia during migraines[38]. Additionally, bilateral damage to LP in rat models significantly increases seizure frequency[39]. We found that selective inhibition of V2M^{Glu} nerve terminals in LP relieved contralateral neuropathic pain, suggesting that this neural circuit is activated following nerve injury and promotes neuropathic pain. The above indicates that the circuitry from V2M^{Glu} to LP mediates, at least in part, the pain modulatory function of V2M^{Glu}. Therefore, V2M^{Glu} and its pathways to the LP may serve as potential targets for the treatment of neuropathic pain, with the former being particularly effective due to its anti-aversive and bilateral analgesic effects.

Previously, we demonstrated that following nerve injury, glutamatergic neurons in the secondary somatosensory cortex, exhibit hyperactivity, which contributes to the development of neuropathic pain[30]. Similarly, the involvement of multiple cortical areas in neuropathic pain has been corroborated by other studies[28,40]. Taken together with these findings, we conclude that the cortex plays a dynamic role in pain modulation through descending pathways, with nerve injury inducing distinct changes in neuronal activity across specific subregions. These alterations collectively contribute to the underlying mechanisms of neuropathic pain. Preclinical research has consistently shown that adjusting neuronal activity in targeted nuclei using optogenetic techniques can alleviate neuropathic pain and its associated negative states. Clinical applications such as repetitive transcranial magnetic stimulation (rTMS) and transcranial direct current stimulation (tDCS) non-invasively modulate cortical neuron excitability and have been used to treat some neuropsychological disorders[41,42]. Given the varied changes and roles of different cortical areas in neuropathic pain, stimulation parameters, based on the specific functions of different cortex, should be relatively adjusted. Therefore, elucidating the role of the cortex in neuropathic pain and its associated circuitry may help identify precise targets and optimize stimulation parameters for rTMS and tDCS treatments. This study further provides a basis for the modulation of neuropathic pain via V2M-encoded visual stimuli. We propose that cortical nuclei may play a crucial role in pain modulation and the development of neuropathic

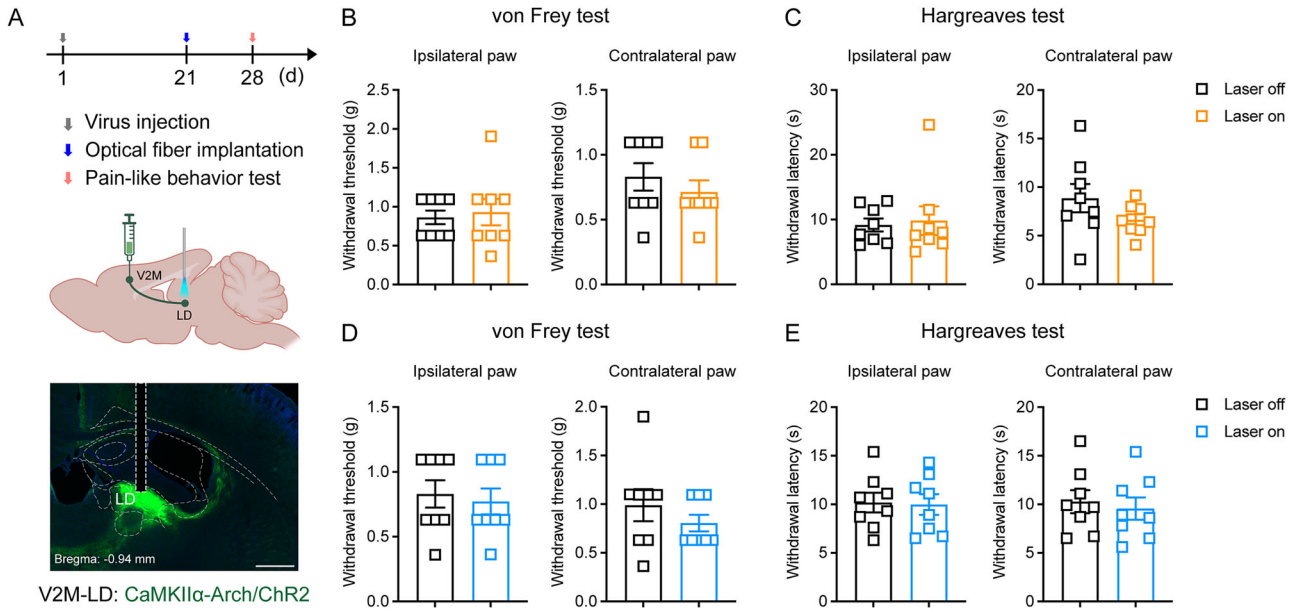

Fig. 7 | Selective inhibition of V2M^{Glu}-LD had no effect to nociception. A Timeline of experimental procedure (upper), schematic of sites for virus injection and optical fiber implantation (middle) and photomicrograph showing the expression of eYFP and optical fiber implantation in the LD (lower). **B**, **C** Withdrawal thresholds and withdrawal latency to mechanical and thermal stimulation of bilateral hind paw during optical inhibition of terminals from V2M^{Glu} in LD. **D**, **E** Withdrawal thresholds and withdrawal latency to mechanical and thermal stimulation of bilateral hind paw during optical activation of terminals from V2M^{Glu} in LD. $n = 8$. All data are presented as mean ± SEM.

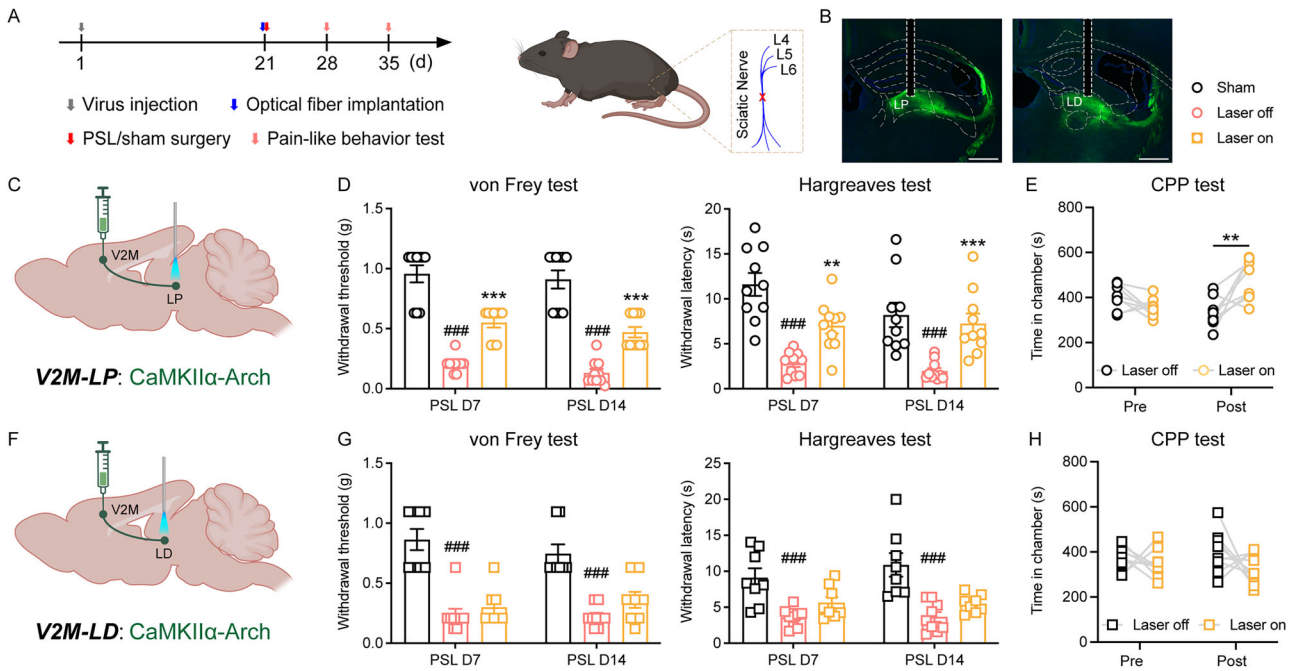

Fig. 8 | Selective inhibition of the circuits from V2M^{Glu} to LP attenuates neuropathic pain. A Timeline of experimental procedure. **B** Representative photomicrograph showing virus carrying eYFP and optical fiber was implanted in the LP or LD. **C** Schematic of sites for virus injection in the V2M and optical fiber implantation in the LP to selectively inhibit V2M^{Glu}-LP circuit. **D** Withdrawal thresholds and withdrawal latency to mechanical and thermal stimulation of bilateral hind paw during optical inhibition of unilateral V2M^{Glu}-LP. $n = 10$. **E** Time spends by the mice in the laser off and laser on paired boxes in pre- and post-conditioning phases in CPP tests. $n = 8$. **F** Schematic of sites for virus injection in the V2M and optical fiber implantation in the LP to selectively inhibit V2M^{Glu}-LD circuit. **G** Withdrawal thresholds and withdrawal latency to mechanical and thermal stimulation of bilateral hind paw during optical inhibition of unilateral V2M^{Glu}-LD. $n = 10$. **H** Time spends by the mice in the laser off and laser on paired boxes in pre- and post-conditioning phases in CPP tests. $n = 9$. Significance was calculated by means of t-test in E and two-way ANOVA with Bonferroni's post hoc test in D, G. $^{**}p < 0.01$ and $^{***}p < 0.001$, respectively, laser on versus laser off in D, G. $^{###}p < 0.001$, sham versus laser off. All data are presented as mean ± SEM.

pain post-nerve injury via their descending projections to the thalamus. Interventions targeting these nuclei and their pathways may show great potential in the treatment of neuropathic pain. Our research provides direct preclinical evidence supporting the value of non-invasive stimulation of V2M for further clinical trials.

In conclusion, this study unveils, for the first time, the significant role of $V2M^{Glu}$ in intrinsic pain modulation. $V2M^{Glu}$ becomes more active following nerve injury, contributing to the maintenance of neuropathic pain. Targeting the $V2M^{Glu}$-LP circuit for inhibition may represent a potential therapeutic avenue for addressing neuropathic pain.

Methods

Animals

Animals used in this study were male C57BL/6J mice aged 8–12 weeks. Mice were obtained from the Shanghai Slack Laboratory Animal Center and housed in the animal facility of the Zhejiang Chinese Medical University with controlled humidity (45–65%) and room temperature (22–24°C) on a standard 12 h light/dark cycle (lights on from 8:30 to 20:30). Standard rodent food and water were available ad libitum. We have complied with all relevant ethical regulations for animal use. This study received ethical approval from the guidelines of the International Association by the Zhejiang Chinese Medical University Animal Experimentation Committee. Efforts were made to ensure minimal animal use and suffering.

Partial sciatic ligation surgery

Partial sciatic ligation (PSL) surgery was performed according to Seltzer et al.[43] Briefly, under isoflurane anesthesia (4% for induction and 2% for maintenance), the right sciatic nerve trunk was surgically exposed under the operating microscope in sterile conditions. An 8-0 thread with a 3/8 curved, reverse-cutting suture needle was inserted into the back of the nerve and bound the thread tightly, ensuring that 1/3 to 1/2 of the nerve on the dorsal side of the nerve trunk was bound in the knot. The sham group exposed the nerve but did not ligate it. Sutured the wound layer by layer. After the procedure, the mice were returned to their cages after recovering from anesthesia.

Delivery of viruses and agents

Mice were anesthetized by sodium pentobarbital (50 mg/kg, i.p.) and mounted on a stereotaxic apparatus. The bregma was exposed by removing the connective tissues from the skull surface. Small craniotomies were then made with a dental drill over the target brain regions. The coordinates relative to bregma for immediate microinjection of virus solution or implantation of fiber optic cannula [core diameter: 200 μm, 0.22 mm numerical aperture (NA); Newdoon, China] into the target brain regions were as follows according to the Paxinos and Franklin (2001) atlas: left V2M (AP: −2.5 mm, ML: +1.2 mm, DV: −0.8 mm), left LP (AP: −1.9 mm, ML: +1.3 mm, DV: −2.5 mm), left LD (AP: −.9 mm, ML: +1.4 mm, DV: −2.5 mm). The cannula was implanted in the target nuclei 3 weeks after virus injection and held in place by dental acrylic, and the patency was maintained with an occlusion stylet. For intracerebral microinjection, a thin glass capillary connected to a 1 mL micro-syringe mounted on an Ultra Micro Pump (World Precision Instruments, USA) was slowly lowered into the target sites. For optical activation or inhibition of V2M glutamatergic neurons and terminals, pAAV-CaMKIIα-hChR2(H134R)-eYFP (1.7×10^{13} vg/ml, 200 nl; OBIO, China;) or pAAV-CaMKIIα-eArch3.0-eYFP (1.3×10^{12} vg/m, 200 nl; OBIO) was infused into the target areas 10 nL/minute of C57BL/6J mice. The glass capillary was left in place for an additional 5-min post-injection to facilitate virus particle diffusion and minimize reflux along the injection track. Animals were kept for 3 to 4 weeks after virus injection to allow maximal viral expression before subsequent experiments. Cannula placement and sites of viral expression were histochemically verified on cryogenic brain sections at the conclusion of each experiment. The core of viral expression was expected to reside within the target nuclei, as per the brain atlas, and align with the cannula tips. Animals exhibiting misaligned sites were excluded from all analyses. To observe the instant effect of optical activation or inhibition of neurons, persistent laser stimulation at 473 nm (blue, power 5 mW, frequency 20 Hz, pulse width 10 ms) or 594 nm (yellow, 5 mW, direct current) was supplied by BL473T3-050 laser or YL589T3-050 laser during the behavioral testing. For activating local glutamatergic neurotransmission, 0.5 μL mixed solution containing AMPA (a glutamate AMPA receptor agonist, 0.5 μg; Sigma-Aldrich) and NMDA (a glutamate NMDA receptor agonist, 0.5 μg; Sigma-Aldrich), was infused into LP slowly over a period of 2 min via a 33-gauge needle that fits the guide cannula. Behavioral tests were performed 15 min later after drug administration.

Behavioral assessments

All behavioral tests were carried out by a blinded examiner in a sound-proof room. Mice were allowed to habituate to the environment in the testing apparatus or room for at least 30 min before behavioral assessment.

Von Frey tests were used to test the noxious mechanical stimulus-evoked pain-like behavior of the hind paw, the mice were placed in a test cage with a metal mesh bottom (8 cm in diameter and 9 cm in height). A set of von Frey filaments (North Coast Medical, Gilroy, CA) numbered 2 to 9 (bending force from 0.02 g to 1.4 g) was applied to deliver mechanical stimulation on the sole surface of the hind paw for 3 s. Tests started with the filament number 5 (0.16 g) and progressed according to the up-down method. Each test constituted a constant number of 5 trials with an interval of at least 5 min between adjacent trials. Sharp withdrawal or immediate flinch of the hind paw indicated a positive reaction. The paw withdrawal threshold (PWT) was calculated using the value of fiber filament sequenced for the fifth stimulation, adding the adjustment factor (±0.5) in each test. The adjustment factor was positive if there was no response to the fifth filament and negative if there was a response. Convert the serial number of the fiber to the corresponding number to force (F) and calculate PWT by substituting the following formula: $PWT = 10^{(0.24*F-2)}$, as described in the previous study[44].

Hargreaves tests were used to test the noxious thermal stimulus-evoked pain-like behavior of the hand paw, the mice were placed in a transparent Plexiglas chamber with a glass bottom ($20 \times 20 \times 14\ cm^3$). A radiant heat source (Ugo Basile, Italy) with an intensity of 20 W was positioned underneath the bottom of the glass and aligned with the plantar surface of the hind paw. The paw withdrawal latency (PWL) to a withdrawal response such as licking, flicking, or lifting the hind paw evoked by thermal stimulation was automatically recorded. The minimum and maximum latencies were set to 1 and 20 s, respectively. Each hind paw was repeated at least 15 min apart, and the average of the two trails was used as the final PWL to heat stimulation.

Real-time place preference (RTPP) is an experiment that measures the effects of optogenetic manipulation based on the subjective behavior of mice approaching or avoiding. Mice were placed in a custom-made three-chamber apparatus that had distinct stripe patterns. Each mouse was placed in the center and allowed to explore all chambers without light stimulation for 5 min recorded as the pre-stimulation phase. After exploration, the mouse indicated a small preference for one of the two chambers. Subsequently, light stimulation was delivered whenever the mouse entered or stayed in the preferred chamber, and the light was turned off when the mouse moved to the other chamber (stimulation phase) for 5 min recorded as the stimulation phase. Finally, the mouse was allowed to freely explore both chambers without light stimulation for 5 min recorded as a post-stimulation phase. The RTPP location plots and total time on the stimulated side were recorded and counted with the ANY-maze software via a digital camera (Logitech, Switzerland).

Conditioned place preference (CPP) was utilized to evaluate the effect of photogenetic modulation to mice after PSL surgery. The CPP apparatus is a standard three-box apparatus comprising two chambers of equal size but with different interior decorations, connected by an intermediate area. During the habituation phase for two days, the mice were placed in the apparatus for 30 min each day and were allowed to move freely with access to all three boxes. On the second day, the movements of each animal in the

first 15 min were recorded and analyzed with ANY-maze to verify the absence of preference for each box. Animals spending > 80% or < 20% of the total time in any box were excluded from further testing. Then, a two-day conditioning experiment was then performed. On the morning of the third day, the mice were placed into the chamber on one side and paired without laser stimulation. After 4 h, they were transferred to the other chamber and exposed to laser stimulation. On the morning of the fourth day, the mice were placed in the chamber associated with laser stimulation, followed by a transfer to the chamber without laser stimulation after 4 h. Each pairing phase lasted 30 min, and the mice were not allowed to access other chambers in the meantime. Finally, on the fifth day, the mice were placed in the interconnecting area with unrestricted access to both boxes, while their movements were recorded for 15 min and analyzed with ANY-maze software. The time that the animal spent in each box and the percentage occupancy (preference) and shifts in occupancy for one side were analyzed by ANY-maze and compared with that on the second day.

In vivo single-unit recordings

Mice anesthetized with 20% urethane (1.4 g/kg i.p., Sigma-Aldrich, Germany) were mounted on a stereotactic frame. A small craniotomy was performed over the left V2M. To investigate the effect of nerve injury on the activity of V2M glutamatergic neurons, a recording microelectrode bundle consisting of 8 channels of wires (diameter 25 mm, A-M systems, Sequim, WA) with impedances of 1–2 MΩ was slowly lowered to the target region by a micromanipulator, recording the spontaneous and stimulus-induced firing of V2M glutamatergic neurons after PSL. Acquisition and analysis of data from single-unit recordings were conducted as previously described[45]. In short, signals were acquired by a multichannel acquisition system (Blackrock Microsystems, Canada) with a sampling rate of 30 kHz and were high- and low-passed at 250 Hz and 7.5 kHz, respectively. Units were selected if the signal-to-noise voltage threshold was 3:1. Recordings were analyzed by Offline Sorter (Plexon, USA) and NeuroExplorer 4.0 (NEX, Colorado Springs). Putative glutamatergic neurons were identified by their wide spike waveform (full width at half maximum 0.30 ms) and sharp autocorrelation[46,47]. The spontaneous and evoked firing of left $V2M^{Glu}$ was recorded 14 d after sham or PSL operation. The spontaneous firing was recorded for 2 min before recording the evoked firing by noxious pinch stimulation. Pinch stimulation was applied by clipping the paw for 30 s using a toothed plastic clip. The firing frequency was recorded both before and during stimulation, and responses were categorized into three distinct types: increase, decrease, or no change. An increase or decrease was defined as a change in firing frequency of at least 20% during stimulation compared to the baseline period. In each stimulation trial, the brush was applied initially, and only after the firing frequency returned to baseline was the pinch applied. When multiple trials were conducted on a single animal, a minimum interval of 15 min was maintained between trials.

Fiber photometry recordings

The calcium activity detecting virus AAV2/8-mCaMKIIα-GCAMP6s-WPRE-pA (7.05×10^{12} vg/ml; 200 nl; Taitool, China) was infused into the left V2M. Three weeks later, an optic fiber placed in a ceramic ferrule was inserted into the V2M. The mice were housed individually for at least 1 week for recovery. For the fiber photometry recording system (Thinkertech, China), the excitation light (488 nm) emitted by the light source was reflected through a dichroic mirror, which was focused with a 10× objective lens (NA = 0.3; Olympus, Japan) and then coupled to the core face of the optical fiber jumper (core diameter 220 μm, numerical aperture 0.37, Inper, China). GCaMP fluorescence was filtered using a GFP bandpass filter and collected using a photomultiplier tube (R3896, Hamamatsu, Japan). The amplifier converted the PMT current output into a voltage signal that was further filtered by a low-pass filter (4 Hz cutoff; Brownlee, USA). The analog voltage signals were digitized at 500 Hz and recorded. The mice were connected to a fiber photometry recording system after being acclimated in a test cage with a wire mesh at the bottom. After the baseline signals were stabilized and recorded for 30 s, mechanical stimulation (1.0 g von Frey filaments, 2 s), thermal stimulation (Hargreaves apparatus, 1 s), and notional stimulation (pinch, 5 s) was given to the ipsilateral hind paws to observe the change of calcium signal. Photometry data were exported as MATLAB files for further analysis. We derived the values of fluorescence change (ΔF/F) by calculating (F-F0)/F0, where F0 is the averaged fluorescence over the 30 s baseline period. ΔF/F values for each mouse were presented as heatmaps, and the averaged values were presented in plots with the SEM indicated by a shaded area.

Immunohistochemistry

Mice were deeply anesthetized with pentobarbital sodium (100 mg/kg, i.p.), and perfused with ice-cold PBS, followed by 4% paraformaldehyde (PH 7.4). The brain was postfixed overnight in the same fixation conditions and dehydrated in 30% sucrose for 48 h at 4 °C. Coronal brain slices (30 μm) were cut with a cryostat (Thermo, USA) and stored in a −80°C freezer. To visualize viral expression, brain slices were washed three times with PBS for 5 min each and mounted with DAPI (36308ES20, Yeasen, China). Fluorescent images were observed and captured by a fluorescence microscope (Olympus, Japan). To determine c-fos expression and assess co-localization with glutamate/ GABAergic neurons, brain slices were first incubated with 0.1% Triton X-100 for 15 min at room temperature (RT) and then incubated with 5% donkey serum albumin for 2 h. Next, the slices were incubated with mouse anti-c-Fos (1:800, Abcam, catalog #ab208942) and rabbit anti-glutamate (1:1000, Sigma-Aldrich, catalog #G6642)/rabbit anti-GABA (1:100, Sigma-Aldrich, catalog #A2052) overnight at 4 °C, then with donkey anti-mouse IgG-Alexa 488 (1:800, Abcam, catalog #ab150105) or donkey anti-rabbit IgG-Alexa-647 (1:800, Abcam, catalog #ab150075) for 2 h at RT. After several wash steps with PBS, slides were mounted with DAPI, and images were captured by a confocal laser scanning microscope (Leica, Germany).

Statistics and Reproducibility

All data are presented as mean ± SEM. Statistical analysis was conducted by GraphPad Prism 8 (GraphPad Software, USA). Shapiro-Wilk test was used to assess whether the data followed a normal distribution. Two-tailed paired or unpaired Student's *t*-tests were used to compare two groups normally distributed, whereas a Mann-Whitney test was used instead of those not normally distributed. One-way analysis of variance (ANOVA) with Dunnett or Tukey or Kruskal-Wallis post hoc tests were used while the Dunn's post hoc was used for the comparison of more than two groups with one factor. When comparing thresholds to thermal or mechanical stimulation among groups, a two-way ANOVA with Bonferroni post hoc multiple comparisons test was used. The significance level was set at $P < 0.05$. Experiments were repeated three times to ensure reproducibility of results. Biological replicates were defined as independent animals or separate neurons. The number of biological replicates (n) is indicated in the figure legends. Data were considered reproducible when similar results were obtained across different replicates.

Data availability

All data supporting the findings of this study are available within the paper and its Supplementary Information. The datasets have been deposited in the Zenodo (https://doi.org/10.5281/zenodo.14942249) (ref. 48).

Received: 19 December 2024; Accepted: 3 March 2025;
Published online: 11 March 2025

References

1. Smith, E. S. J. Advances in understanding nociception and neuropathic pain. *J. Neurol.* **265**, 231–238 (2018).
2. van Hecke, O., Austin, S. K., Khan, R. A., Smith, B. H. & Torrance, N. Neuropathic pain in the general population: A systematic review of epidemiological studies. *Pain* **155**, 654–662 (2014).
3. Jensen, T. S. & Finnerup, N. B. Allodynia and hyperalgesia in neuropathic pain: clinical manifestations and mechanisms. *Lancet Neurol.* **13**, 924–935 (2014).

4. Cohen, S. P. Neuropathic pain: mechanisms and their clinical implications (vol 348, f7656, 2014). *BMJ-Br. Med. J.* **348**, f7656 (2014).
5. Bannister, K., Sachau, J., Baron, R. & Dickenson, A. H. Neuropathic Pain: Mechanism-Based Therapeutics. *Annu. Rev. Pharmacol. Toxicol.* **60**, 257–274 (2020).
6. Kragel, P. A. et al. Generalizable representations of pain, cognitive control, and negative emotion in medial frontal cortex. *Nat. Neurosci.* **21**, 283 (2018).
7. Lee, M. et al. Activation of Corticostriatal Circuitry Relieves Chronic Neuropathic Pain. *J. Neurosci.* **35**, 5247–5259 (2015).
8. Gadotti, V. M., Zhang, Z., Huang, J. & Zamponi, G. W. Analgesic effects of optogenetic inhibition of basolateral amygdala inputs into the prefrontal cortex in nerve injured female mice. *Mol. Brain* **12**, 105 (2019).
9. Tan, L. L. & Kuner, R. Neocortical circuits in pain and pain relief. *Nat. Rev. Neurosci.* **22**, 458–471 (2021).
10. Barthas, F. et al. The anterior cingulate cortex is a critical hub for pain-induced depression. *Biol. Psychiatry* **77**, 236–245 (2015).
11. Lu, C. et al. Insular Cortex is Critical for the Perception, Modulation, and Chronification of Pain. *Neurosci. Bull.* **32**, 191–201 (2016).
12. Cheng, K., Martin, L. F., Slepian, M. J., Patwardhan, A. M. & Ibrahim, M. M. Mechanisms and Pathways of Pain Photobiomodulation: A Narrative Review. *J. Pain.* **22**, 763–777 (2021).
13. Hou, T.-W., Yang, C.-C., Lai, T.-H., Wu, Y.-H. & Yang, C.-P. Light Therapy in Chronic Migraine. *Curr. Pain. Headache Rep.* **28**, 621–626 (2024).
14. Hu, Z. et al. A visual circuit related to the periaqueductal gray area for the antinociceptive effects of bright light treatment. *Neuron* **110**, 1712 (2022).
15. Wu, X.-Q. et al. Glutamatergic and GABAergic neurons in the vLGN mediate the nociceptive effects of green and red light on neuropathic pain. *Neurobiol. Dis.* **183**, 106164 (2023).
16. Salzmann, M. F. V., Bartels, A., Logothetis, N. K. & Schuez, A. Color Blobs in Cortical Areas V1 and V2 of the New World Monkey Callithrix jacchus, Revealed by Non-Differential Optical Imaging. *J. Neurosci.* **32**, 7881–7894 (2012).
17. Filippi, P. M., Messina, R., Rocca, M. A., Goadsby, P. J. & Filippi, M. Insights into migraine attacks from neuroimaging. *Lancet Neurol.* **22**, 834–846 (2023).
18. Monaco, S., Malfatti, G., Culham, J. C., Cattaneo, L. & Turella, L. Decoding motor imagery and action planning in the early visual cortex: Overlapping but distinct neural mechanisms. *Neuroimage* **218**, 116981 (2020).
19. Van der Gucht, E., Jacobs, S., Kaneko, T., Vandesande, F. & Arckens, L. Distribution and morphological characterization of phosphate-activated glutaminase-immunoreactive neurons in cat visual cortex. *Brain Res.* **988**, 29–42 (2003).
20. Zhang, J. et al. c-fos regulates neuronal excitability and survival. *Nat. Genet.* **30**, 416–420 (2002).
21. Gan, Z. et al. Layer-specific pain relief pathways originating from primary motor cortex. *Science* **378**, 1336–1343 (2022).
22. Kuner, R. & Flor, H. Structural plasticity and reorganisation in chronic pain. *Nat. Rev. Neurosci.* **18**, 20–30 (2017).
23. Zhou, W. et al. Sound induces analgesia through corticothalamic circuits. *Science* **377**, 198 (2022).
24. Sasannejad, P. et al. Lavender Essential Oil in the Treatment of Migraine Headache: A Placebo-Controlled Clinical Trial. *Eur. Neurol.* **67**, 288–291 (2012).
25. Stankewitz, A. & May, A. Increased limbic and brainstem activity during migraine attacks following olfactory stimulation. *Neurology* **77**, 476–482 (2011).
26. Goffer, Y. et al. Calcium-Permeable AMPA Receptors in the Nucleus Accumbens Regulate Depression-Like Behaviors in the Chronic Neuropathic Pain State. *J. Neurosci.* **33**, 19034–19044 (2013).
27. Huang, Q., Lin, J., Han, R., Peng, C. & Huang, A. Using Virtual Reality Exposure Therapy in Pain Management: A Systematic Review and Meta-Analysis of Randomized Controlled Trials. *Value Health* **25**, 288–301 (2022).
28. Valet, M. et al. Distraction modulates connectivity of the cingulo-frontal cortex and the midbrain during pain–an fMRI analysis. *Pain* **109**, 399–408 (2004).
29. Collins, D. P., Anastasiades, P. G., Marlin, J. J. & Carter, A. G. Reciprocal Circuits Linking the Prefrontal Cortex with Dorsal and Ventral Thalamic Nuclei. *Neuron* **98**, 366 (2018).
30. Prasad, J. A., Carroll, B. J. & Sherman, S. M. Layer 5 Corticofugal Projections from Diverse Cortical Areas: Variations on a Pattern of Thalamic and Extrathalamic. *J. Neurosci.* **40**, 5785–5796 (2020).
31. Monconduit, L., Lopez-Avila, A., Molat, J.-L., Chalus, M. & Villanueva, L. Corticofugal output from the primary somatosensory cortex selectively modulates innocuous and noxious inputs in the rat spinothalamic system. *J. Neurosci*. **26**, 8441–8450 (2006).
32. Park, A., Li, Y., Masri, R. & Keller, A. Presynaptic and extrasynaptic regulation of posterior nucleus of thalamus. *J. Neurophysiol.* **118**, 507–519 (2017).
33. Leow, Y. N. et al. Brain-wide mapping of inputs to the mouse lateral posterior (LP/Pulvinar) thalamus-anterior cingulate cortex network. *J. Comp. Neurol.* **530**, 1992–2013 (2022).
34. Scholl, L. R., Foik, A. T. & Lyon, D. C. Projections between visual cortex and pulvinar in the rat. *J. Comp. Neurol.* **529**, 129–140 (2021).
35. Aggleton, J. P. & Nelson, A. J. D. Why do lesions in the rodent anterior thalamic nuclei cause such severe spatial deficits? *Neurosci. Biobehav. Rev.* **54**, 131–144 (2015).
36. Grieve, K. L., Acuna, C. & Cudeiro, J. The primate pulvinar nuclei: vision and action. *Trends Neurosci.* **23**, 35–39 (2000).
37. Wei, P. et al. Processing of visually evoked innate fear by a non-canonical thalamic pathway. *Nat. Commun.* **6**, 6756 (2015).
38. Kagan, R., Kainz, V., Burstein, R. & Noseda, R. Hypothalamic and basal ganglia projections to the posterior thalamus: possible role in modulation of migraine headache and photophobia. *Neuroscience* **248**, 359–368 (2013).
39. de Freitas Sonoda, E. Y., Cysneiros, R. M., Arida, R. M., Cavalheiro, E. A. & Scorza, F. A. Activation and involvement of the lateral-posterior nucleus of the thalamus after a single generalized tonic-clonic seizure. *Epilepsy Behav.* **28**, 104–107 (2013).
40. Wrigley, P. J. et al. Neuropathic pain and primary somatosensory cortex reorganization following spinal cord injury. *Pain* **141**, 52–59 (2009).
41. Stagg, C. J., Antal, A. & Nitsche, M. A. Physiology of Transcranial Direct Current Stimulation. *J. ECT* **34**, 144–152 (2018).
42. Hoogendam, J. M., Ramakers, G. M. J. & Di Lazzaro, V. Physiology of repetitive transcranial magnetic stimulation of the human brain. *Brain Stimul.* **3**, 95–118 (2010).
43. Seltzer, Z. E., Dubner, R. & Shir, Y. A novel behavioral model of neuropathic pain disorders produced in rats by partial sciatic nerve injury. *Pain* **43**, 205–218 (1990).
44. Bonin, R. P., Bories, C. & De Koninck, Y. A simplified up-down method (SUDO) for measuring mechanical nociception in rodents using von Frey filaments. *Mol. Pain.* **10**, 26 (2014).
45. Wang, Y. et al. Depolarized GABAergic Signaling in Subicular Microcircuits Mediates Generalized Seizure in Temporal Lobe Epilepsy. *Neuron* **95**, 92 (2017).
46. Csicsvari, J., Hirase, H., Czurko, A., Mamiya, A. & Buzsaki, G. Oscillatory coupling of hippocampal pyramidal cells and interneurons in the behaving Rat. *J. Neurosci.* **19**, 274–287 (1999).
47. Van Quyen, M. L. et al. Cell type-specific firing during ripple oscillations in the hippocampal formation of humans. *J. Neurosci.* **28**, 6104–6110 (2008).
48. Chen, Z. et al. A glutamatergic innervation from medial area of secondary visual cortex to lateral posterior thalamic nucleus

facilitates nociceptive and neuropathic pain. Zenodo https://zenodo.org/records/14942249 (2025).

Acknowledgements
We acknowledge BioRender (https://biorender.com/) for providing the tools to create the graphical abstract in this manuscript. This study was supported by grants from the National Natural Science Foundation of China 82304459 (YD)/82104136 (TTH), and a project supported by the Scientific Research Fund of Zhejiang Provincial Education Department Y202454988 (BT).

Author contributions
Conceptualization: Z.C., Y.D. and J.Y. Data curation: B.T., X.Q.W., Y.L.D., and C.R.Y. Formal analysis: B.T., X.Q.W., Y.L.D., C.R.Y. and Y.J. Writing - original draft: B.T., X.Q.W., Y.D., C.R.Y. and Y.J. Writing - review & editing: B.T., X.Q.W., Y.L.D., C.R.Y., C.L.X., J.Y., T.T.H., Y.D. and Z.C. Supervision: Z.C.

Competing interests
The authors declare no competing interests.

Additional information
Supplementary information The online version contains supplementary material available at https://doi.org/10.1038/s42003-025-07874-7.

Correspondence and requests for materials should be addressed to Zhong Chen.

Peer review information *Communications Biology* thanks the anonymous reviewers for their contribution to the peer review of this work. Primary Handling Editor: Jasmine Pan.